

## SOLAR DRYING OF SLUDGE OF BIOFOULING WASHING COMING FROM THE AQUACULTURE INDUSTRY

---

### *R. Poblete*

Universidad Católica del Norte, Facultad de Ciencias del Mar Escuela de Prevención de Riesgos y Medioambiente, Coquimbo, Chile  
Núcleo Gestión Avanzada de Residuos y Energías Renovables

### *L. A. Valencia-Ceballo*

Centro de Investigación en Materiales Avanzados, S.C., Unidad Durango, México

### *E. Cortes*

Universidad Católica del Norte, Facultad de Ciencias del Mar Escuela de Prevención de Riesgos y Medioambiente, Coquimbo, Chile  
Núcleo Gestión Avanzada de Residuos y Energías Renovables

### *J. A. Munizaga-Plaza*

Universidad Católica del Norte, Facultad de Ciencias del Mar Escuela de Prevención de Riesgos y Medioambiente, Coquimbo, Chile  
Núcleo Gestión Avanzada de Residuos y Energías Renovables  
Department of Earth and Environmental Sciences, Ludwig Maximilians Universität, Munich, Germany

All content in this magazine is licensed under a Creative Commons Attribution License. Attribution-Non-Commercial-Non-Derivatives 4.0 International (CC BY-NC-ND 4.0).



**Abstract:** The sludge produced in the aquaculture industry has an amount of moisture traditionally dried using the open sun drying method, which results in problems such as rewetting during rainfall events, the arrival of vectors and pollution. It is the first research where has been studied the use of a solar air heater with fins of different heights, a single and double-pass solar air heater and different thermal storage materials to enhance the efficiency of a solar dryer for drying sludge coming from the culture of *Argopecten purpuratus*, as a sustainable energy strategy. When using higher fins, the solar air heater requires less solar energy. With 8 cm high fins, the sludge got a constant mass when 58,567 kJ of solar energy was received in the dryer. When the height of the fins was 6, 4, and 0, a complete dried sludge was obtained with 71,394; 71,255; and 92,523 kJ of accumulative solar energy, respectively. Fin size variations result in significant differences in the drying process.

The highest performance of the solar air heater was obtained with the run involving 8 cm high fins, and the performance decreased as the fins got smaller. The performance results were 6.7%, 11.0%, 21.2% and 27.9% for heights of 0, 4, 6 and 8 cm, respectively.

In the evaluation of single and double pass in the solar air heater, the first one gets at the exit of the device 3.48 °C above environmental temperature, with an average thermal efficiency of 8.51% and the double pass SAH get an output temperature of 5.22 °C above the environmental temperature, and an average thermal efficiency was 16.53%.

Also, different materials were evaluated as thermal storage, obtaining thermal efficiencies for heat storage were 0.88 for sand in aluminium cans, 0.49 for pebbles and 0.48 for rocks. Using these materials in a thermal storage system maintains the output temperature above the input temperature

when there is low or null solar radiation. The thermal storage system permits a higher moisture reduction ever after before the sunshine, promoting a dry in the non-sunny hours.

**Keywords:** Sludge drying; solar dryer; solar air heater; thermal storage.

## INTRODUCTION

Aquaculture is essential in producing seafood worldwide, and rapidly expanding to respond to increasing demands is expected (Straume et al., 2020). One of the most important species for aquaculture in Chile and Peru is the native bivalve scallop *Argopecten purpuratus* (Kluger et al., 2019), placed in the local biota where upwelling-influenced habitats of Humboldt Current System reside (Ramajo et al., 2020).

Biofouling is one of the critical ecological problems for submerged objects in aquaculture, including scallop culture, negatively impacting the flotation of polyethylene plastics (Bera et al., 2018). Biofouling decreases the water flow across submerged aquaculture systems (Jeong et al., 2021), that is, lanterns and pearl nets, and results in severe difficulties in aquaculture because it harms the operation and structural integrity (Nobakht-Kolur et al., 2021).

High-pressure washing machines are used to remove fouling from the culture systems. They consume a large amount of water (Comas et al., 2021), producing a large quantity of sludge that needs to be managed as industrial waste (Bannister et al., 2019).

On the one hand, the drying process requires a high amount of energy and is generally expensive (Di Fraia et al., 2016); on the other hand, direct solar drying of materials is the oldest way of removing water. However, there are several related problems, such as the rewetting during rainfalls, winds, the arrival of vectors (mice, insects, birds) and pollution; these problems motivate the use of industrial

and intensive methods that require equipment that requires electrical energy or fossil fuels as a source of heat, with high operational costs (Rezaei et al., 2022).

It was investigated using a solar roof as in the sewage sludge drying process using a sandwich-like chamber bed (Wang et al., 2019). The drying behaviour and energy demand of a microwave system applied in sludge drying were investigated, considering the process's exposure time, drying rate, and specific energy consumption (Kocbek et al., 2020).

The thermal storage systems allow recovery of the excess solar energy in sunny hours and deliver this energy after sunset, permitting a continuous process (Gilago et al., 2023). In the research of our investigation group, we evaluated the improvement of solar drying of sludge from a landfill utilising thermal storage systems consisting of a rock bed with air heated in a solar air heater (SAH) (Poblete & Painemal, 2020).

SAH consists of a glazing unit, a bottom plate, an absorber plate, and inlet and outlet sections that allow airflow and thermal energy transfer to this flow. Results showed that a solar air heater with a double glass cover performs better than a solar air heater with a single glass cover (Prakash et al., 2022).

This heat transfer is enhanced by placing fins on the absorber plate to avoid the formation of a laminar sub-layer and the generation of turbulence due to flow separation phenomena (Surendhar et al., 2022)(Surendhar et al., 2022; Saravanakumar et al., 2020a). Research shows that the use of fins has a significant impact on thermal performance depending on their geometry and flow parameters (A. Kumar et al., 2017), where the height-to-duct hydraulic diameter ( $e/D_h$ ) ratio and relative roughness pitch ( $p/e$ ) are fundamental (Goel et al., 2021).

To the best of our knowledge, no scientific

research has focused on the solar drying of sludge from aquaculture processes. Therefore, in this research, we evaluated the use of fins with different geometries in a SAH and different materials in a thermal storage system as a novel process to dry sludge from the industrial culture of scallops, being this the first work carried out to investigate this issue with a focus on a sustainable energy strategy.

## 2.- Materials and Methods

Different configurations used in the culture of **A. purpuratus** for enhancing the performance of drying sludge from the washing of lantern systems were evaluated. A 50 kg sample of sludge was taken from the rotary drum filter used for the industrial wastewater from washing culture lanterns in Coquimbo, Chile. The main characteristics of the sludge are given in Table 1.

Parameter	Sludge	Method
Density (kg/L)	1.25	Gravimetric
Moisture (%)	75	Wet base
pH	7.95	pH-meter
Conductivity (mS/cm)	44.6	ISE
Copper (mg/L)	3.6	TR-ICPMS
Iron (mg/L)	1.05	TR-ICPMS
Cadmium (mg/kg)	29.4	TR-ICPMS

Table 1. The main characteristics of the sludge originated from the washing of the culture, *A. purpuratus*, and the water recovered

The industrial wastewater from the washing of these lanterns, the primary water treatment, and the sludge produced are shown in Figure 1:



Figure 1. Photos of: a) lanterns to be washed; b) primary wastewater systems; and c) storage of generated sludge.

## EVALUATION OF THE SIZE OF THE FINS OF THE SAH

The use of different sizes of fins in a SAH of one path that heated the air at the entrance of the solar dryer was evaluated, to be then applied to the drying of the industrial sludge. Fig. 2 depicts a schematic diagram of the solar dryer, SAH, and collector used for sludge drying. These devices are described in (Poblete & Painemal, 2018). The solar dryer [18][18] has lateral and frontal walls and a polycarbonate sunroof, with a heat transfer coefficient of  $3.8 \text{ W/m}^2\text{°C}$  and optical transmittance of 80%. An air extractor (20 W) on the wooden back wall removes the vapour generated in the drying process. The air that entered the solar dryer was heated using a SAH, as shown in Figure 2, with a velocity of 1 m/s, measured in the duct at the device's exit. The SAH consists of a rectangular wooden base ( $0.96 \text{ m}^2$ ) with side walls made of wood (10 cm high) and two horizontal glass roofs (4 mm thick). Inside the SAH are vertical fins made of glass to enhance air turbulence and heat transfer. Air temperature and velocity were determined using a thermo-anemometer (model D8060048, Veto Cia. Ltda.).

The solar energy received by the systems ( $rad_{g,n}$ ,  $\text{W/m}^2$ ) was determined using a pyranometer (CPM 10, Kipp & Zonen; 285-2,800 nm wavelength) which was tilted to  $30^\circ$ , as the latitude of the testing place (Coquimbo, Chile).

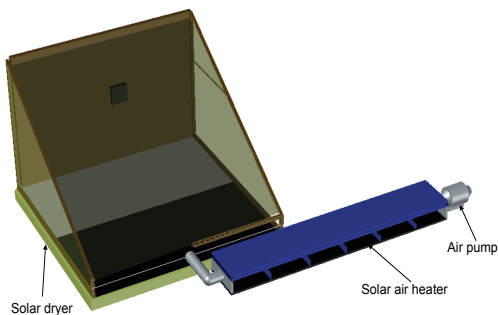


Figure 2. Schematic diagram of the solar systems used to dry the aquaculture sludge.

We evaluated three different heights ( $e$ ) of rectangular fins in the SAH, which were placed in the air path inside the SAH. There were five fins 40 cm wide ( $W$ ), 1 cm thick, and 4 cm (run 1), 6 cm (run 2), or 8 cm (run 3) high, and the system was also evaluated without fins as control ( $e=0$ ) (run C). Figure 3 shows the SAH and the device's geometry schematic diagram. The pitch ( $p$ ) between the fins was 0.4 m.

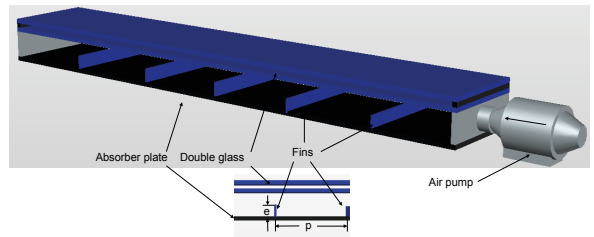


Figure 3. Geometry and schematic diagram of the SAH.

Three runs were performed, one for each fin height. During each run, 500 g of sludge was placed on a stainless-steel tray inside the solar dryer, which had dimensions of 7 cm height and  $450 \text{ cm}^2$  surface area. The tray mass, air temperature (before and after the SAH), and solar drying were recorded. The mass of samples was chosen for ease of handling. The runs continued until the sludge reached a stable mass. The moisture content of the sludge was determined and recorded before commencing the drying process. The moisture ( $M$ ) was determined considering (Prachayawarakorn et al., 2008) using Eq. (1):

$$M = \frac{m_t - d}{d} * 100 \quad (1),$$

where  $m_t$  is the mass of wet sludge at time  $t$ , and  $d$  is the mass of sludge after drying.

The heat obtained ( $Q_u$ ) by the airflow in the SAH, evaluated for each high of fins, was calculated using Eq. (2):

$$Q_u = m * C_p * (T_o - T_{in}) \quad (2),$$

being  $m$  is the mass flow of air (kg/s),  $C_p$  is

the specific heat capacity of air (J/(kg\*K)),  $T_0$  and  $T_{in}$  are the temperatures of the airflow that exits and enters the SAH (K). The performance of the SAH was determined using Eq. (3):

$$\eta_{SAH} = \frac{Q_u}{rad_{g,n} * A} \quad (3)$$

where  $rad_{g,n}$  is the mean solar radiation received by the system (W/m<sup>2</sup>), and A is the SAH (m<sup>2</sup>) area.

The relative roughness pitch P/e that allows for assessing the relation of the geometry of the fins with the drying process was also determined. The Nusselt number (Nu) change was studied using different e values. The Nu obtained in the work of the SAH was calculated by using Eq. (4):

$$Nu = \frac{h_c * D_e}{k_a} \quad (4)$$

where  $h_c$  is the convective heat transfer coefficient (W/(m<sup>2</sup>\*K)),  $D_e$  is the hydraulic diameter of the SAH (m), and  $k_a$  is the thermal conductivity of the fluid (W/(m\*K));  $h_c$  (W/m<sup>2</sup>\*K) was determined using Eq. (5):

$$h_c = \frac{Q_u}{A * (T_p - T_{avg})} \quad (5)$$

$T_p$  is the absorber's average surface temperature (K), and  $T_{avg}$  is the average temperature of air considering  $T_0$  and  $T_{in}$  (K).

Considering that the experiments were realised on different days and with different solar irradiation conditions, the amount of solar irradiation received by the SAH and the solar dryer was measured to compare these results. As well, the accumulative solar energy ( $Q_{rad}$ ) used per unit of mass of sludge (kg/kJ) was determined using [20][20]Eq. 6:

$$Q_{rad,n} \left( \frac{kg}{kJ} \right) = Q_{rad,n-1} + \Delta t_n * rad_{g,n} * \frac{A}{m_t} \quad (6)$$

where  $Q_{rad,n}$  and  $Q_{rad,n-1}$  are the solar energy accumulated per mass of sludge (kJ/kg) at times of measurement  $n$  and  $n-1$ , respectively;  $\Delta_{t_n}$  is time of the measure (s) and  $rad_{g,n}$  is the

mean radiation received on the solar systems (W/m<sup>2</sup>).

The air temperature that enters and exits the SAH and in the solar dryer was measured along the runs using a Campbell Scientific thermocouple, Inc. 109-L34 (0.25 °C accuracy) and recorded in a datalogger Campbell Scientific.

Drying efficiency ( $E_D$ ), that is the relation between the harnessed energy in the removed water present in the sludge and the energy necessary to remove this moisture, was determined based on the solar and electric energy consumed by the equipment involved in the process (air extractor, air pump and recirculation pump), determined using Eq. (7) (P. P. Singh et al., 2006).

$$E_D = \frac{m_w * L}{(P + rad_{g,n} * A_d) * t} \quad (7)$$

where  $m_w$  is the mass of evaporated water from the sludge (kg),  $L$  is the latent heat of vapourisation (J/kg);  $P$  is the sum of the power installed in the process (W) work in the time  $t$  (s);  $m_w$  was calculated using Eq. (8):

$$m_w = \frac{m_i * (M_i - M_f)}{100 - M_f} \quad (8)$$

where  $M_i$  and  $M_f$  are the preliminary and final sludge moistures (kg), respectively.

## 2.2.- Solar air heaters evaluation

Considering the results of the high of fins that produce the best performance, the two SAH designs were tested to select which has the best thermal efficiency. The first one (see Figure 4a) is a single-pass SAH, with external dimensions of 2.34 m long, 0.15 m height, 0.418 m width and 0.89 m<sup>2</sup> of double glass roof, 4 mm thick, for incoming radiation. The five fins inside are glass with a pitch of 0.4 m. The bottom and side walls are made of 2 cm thick wood, covered with black paint. The inlet and outlet air ducts are 0.05 m in diameter. The second one (see Figure 4b) is a double-pass SAH; its external dimensions are 2.425 m long, 0.44 m width, 0.253 m height and 0.965

m<sup>2</sup> of double glass roof for incoming radiation. The high of the fins of the both SAH, single-pass and double-pass, was the best performer in evaluating the size of the fins of the SAH.

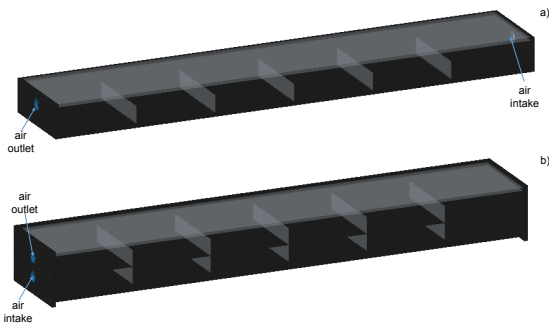


Figure 4. Schematic diagram of SAHs: a) single pass, and b) double pass.

To evaluate the SAHs efficiency, which was calculated using the eq. 3, each design was connected to an air blower (Blauberg, 230 V, 23-25 W, 170-220 m<sup>3</sup>/h) to force air to enter them. A temperature sensor (model AT109 L34, Campbell Scientific, Inc.; ±0.25 °C accuracy) was installed at the air exit of each SAH and the air surrounding the systems. All sensors were connected to a datalogger (model CR300, Campbell Scientific, Inc.) for data registration and collection. A Thermo-anemometer (model D8060048, Veto) measured air velocity, and a pyranometer (CPM 10, Kipp&Zonen; 7 to 14 μV/W/m of sensibility) was utilised to measure the solar radiation.

## MATERIALS THERMAL STORAGE EFFICIENCY TESTS

Once elected the most efficient SAH (single pass or double pass), it was connected to the heat storage container that contained materials to be evaluated as thermal storage. Each thermal storage material (rocks, pebbles and sand inside aluminium cans), all of them without phase change material, was tested for separate in periods of seven days. The TES materials analysed were rocks (19 units with

an average density of 3,443.82 kg/m<sup>3</sup>), pebbles (74 kg with an average density of 2,554.72 kg/m<sup>3</sup>) and sand inside aluminium cans (59 soda cans of 355 ml with an average weight of 0.489 kg per filled can). Each TES material, none of them was a phase change material, was tested separately over seven days.

Figure 5 depicts a diagram of the thermal storage system connected to the SAH and solar dryer.

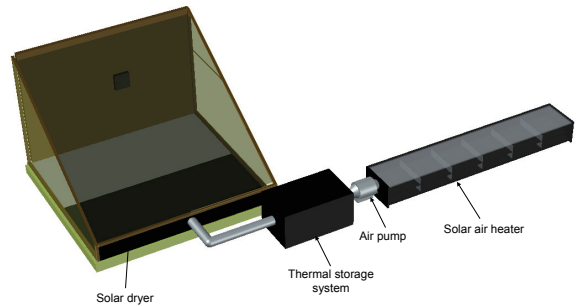


Figure 5. Schematic diagram of the thermal storage system, SAHs and solar dryer.

Thermal storage materials were tested to select the one with the best heat storage efficiency: rocks, pebbles and sand inside aluminium cans.

For the measurements, temperature sensors (model AT109 L34, Campbell Scientific, operating temperature range: -50 °C to 70°C, Inc.; ±0.25°C accuracy) were installed at the input and output of air of the heat storage container.

The thermal storage efficiency for each material was obtained with eq. 9, where the instant heat flux was calculated every 5 minutes with eq. 10. Finally, discharge and charge heat were estimated with eqs.11 and 12, respectively.

$$\eta_{material} = \frac{Q_{discharge}}{Q_{charge}} \quad (9)$$

$$\dot{Q} = \rho_{avg,air} * A_{tube} * V_{air} * Cp_{air} * \Delta T \quad (10)$$

$$Q_{discharge} = \frac{\sum_i^n \dot{Q}}{n} \quad \text{when } \dot{Q} < 0 \quad (11)$$

$$Q_{charge} = \frac{\sum_i^n \dot{Q}}{n} \quad \text{when } \dot{Q} > 0 \quad (12)$$

To determine the influence of the use of a thermal storage system on the solar drying process it was carried out runs with and without this system in the drying of the aquaculture industrial sludge, using the most efficient SAH (single pass or double pass) and the thermal storage material that gets the higher thermal storage efficiency.

Three runs were carried out to perform this analysis, with and without a thermal storage system. For each run, 500 g of the sludge was subjected to the drying process, located on a stainless-steel tray with the exact dimensions used to evaluate the size of the SAH fins inside the solar dryer. Tray mass, air temperature (before and after the SAH) and solar drying were recorded. Each run lasted until the mass of the sludge was stable, and the moisture content of the sludge was determined and stored before the drying process.

An ANOVA evaluation was carried out, with a p-value of 0.05, to determine significant differences in the runs using the different configurations evaluated. A Tukey test was also carried out.

## RESULTS AND DISCUSSION

### EFFECT OF THE SIZE OF THE FINS OF THE SAH IN THE DRYING

Figure 6 presents the change in the moisture of the sludge from lantern systems about the accumulative solar energy ( $Q_{rad}$ ) using different sizes of fins. As can be seen, a smaller amount of solar energy was required when using the SAH with higher fins. When 8 cm high fins were used, sludge got a constant mass and null moisture when 58,567 kJ/kg of solar energy was received in the dryer. When the heights of the fins were 6, 4, and 0, a complete drying was achieved using 71,394, 71,255, and 92,523 kJ/kg of accumulative solar

energy, respectively.  $Q_{rad}$  required using fins is lower than those needed in previous research of our investigation group, where 83,478 kJ/kg of solar energy was used to dry sludge from landfill leachate treatment (Poblete & Painemal, 2020). When higher fins were used, the surface area also increased, and more air reached the contact surface due to vortex phenomena, which enhanced momentum and temperature (Singh & Negi, 2020).

Results show significant differences in the drying process using fins of different sizes, with F values higher than the standardised value ( $4.7353 > 0.00521$ ). The Tukey test shows that there are significant differences between run 1 and C and between run 1 and run 3.

Requiring less solar energy allows adequate drying in a smaller solar dryer, a drying process completed in a shorter time or the execution of the work in a place with low solar radiation intensity.

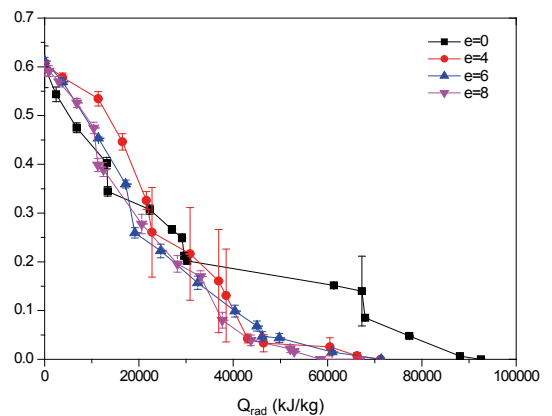


Figure 6. Change in moisture content of samples using fins with different heights. Error bars symbolise the standard deviation of the results (n=3)

The variations in the drying process results are linked to the SAH's performance, which is responsible for heating the air entering the solar dryer. Figure 7a illustrates that the SAH run with 8 cm high fins achieved the highest performance, while performance decreased with smaller. Performance results were 6.7%,

11.0%, 21.2% and 27.9% for fin heights of 0, 4, 6 and 8 cm, respectively. This enhancement in the performance of the SAH is also related to the Nusselt number (Figure 7b), which involves the thermal conductivity of air, the convection heat transfer ( $h_c$ ) (Figure 7c), and the hydraulic diameter of the SAH (Yadav et al., 2022). An increase in Nu and  $h_c$  values were observed when higher fins were used.

The increase in Nu can be attributed to the disruption created by the fins in the viscous sub-layer, which allows reducing the boundary layer and the rising heat transfer, resulting in a higher  $h_c$  (Surendhar et al., 2021), which is proportional to Nu.

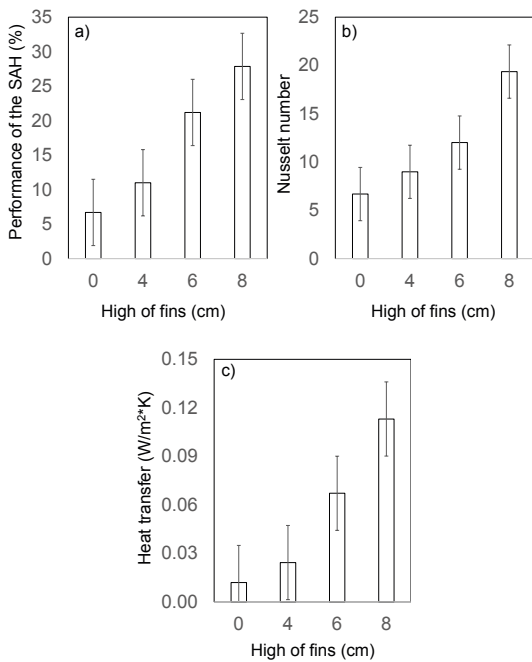


Figure 7. a)  $\eta_{SAH}$ , b) Nusselt, and c)  $h_c$  of the SAH with fins of different heights (e). Error bars symbolise the standard deviation of the results (n=3)

An increase in the size of the fins produces a significant increase in thermal efficiency since more turbulence is created inside the SAH and due to the formation of a secondary flow that takes more thermal energy, enhancing the heat transfer to the air (Saravanakumar et al., 2019). In this research, they reported

an enhancement in the efficiency of a SAH when fins were used due to an enhancement in the convection heat transfer coefficient and a larger heat transfer area. Also, they observed that the larger the fins, the higher the efficiency, getting a maximum enhancement of 28.3% for fins of 0.015 m.

The performance of the SAH and the drying of sludge depends on the solar radiation and the temperature of the air inside it, considering that a dryer with high efficiency allows removing moisture using a lower amount of energy. The drying efficiency obtained in the present study was higher than that reported by (Poonia et al., 2022) and (Mugi et al., 2022), who got an efficiency of 18.0% and 11.65%, respectively.

Results show significant differences in the drying efficiency of the runs carried out using fins with different sizes, with F values higher than the standardised value ( $4.50512 > 0.00738$ ). The Tukey test shows significant differences in the drying efficiency between run three and one and between run three and two. These results coincide with those shown in Figure 4, where it is possible to observe that run 3 (e=8 cm) gets stable moisture using less accumulated solar energy than in the other runs.

The relative roughness pitch (p/e) of the configurations studied in this research, which involve the size of the fins and the distance between them, was 10, 6.7 and 5, for e of 4, 6 and 8 cm, respectively. For the experiment without fins (e=0), the p/e is undefined. These values are like those provided by (Saravanakumar et al., 2020b), who use a p/e of 10, applied to evaluate the exergetic performance and optimisation of a SAH.

## SOLAR AIR HEATERS EVALUATION

Figures 8 and 9 show temperatures and thermal efficiencies obtained using single-pass or double-pass SAH, respectively. SAH designs were tested simultaneously in two weeks in August 2022, the winter season in Chile. The maximum and average radiation in the period were  $758.1 \text{ W/m}^2$  and  $231.5 \text{ W/m}^2$ , respectively. The maximum temperature was  $20.85 \text{ }^\circ\text{C}$ , and the average was  $12.88 \text{ }^\circ\text{C}$ . At the single pass SAH, the output temperature reached  $60.47 \text{ }^\circ\text{C}$  and maintained an average output temperature of  $16.37 \text{ }^\circ\text{C}$ , which means  $3.48 \text{ }^\circ\text{C}$  above environmental temperature, with a computed average thermal efficiency of  $8.51\%$ . While at double pass SAH, the maximum temperature accounted for  $52.6 \text{ }^\circ\text{C}$ . Its average output temperature was  $18.11 \text{ }^\circ\text{C}$ , which means  $5.22 \text{ }^\circ\text{C}$  above the environmental temperature, and its average thermal efficiency was  $16.53\%$ . The difference in the temperature and thermal efficiency is due to the higher time of contact between the air and the absorber plate of the SAH of the double-pass, enhancing the heat transfer (Kashyap et al., 2023), forming higher turbulence in the pass (Kumar et al., 2023), and also the use of a double-pass allows for reduced thermal losses through the cover, because of a due to higher utilisation of this heat by the air (Pachori et al., 2023).

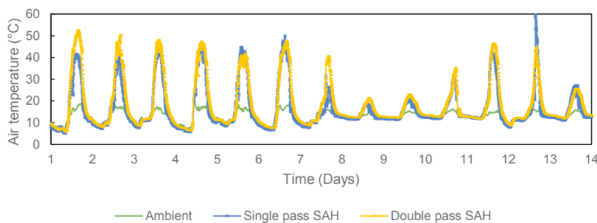


Figure 8. Comparison of air temperatures at the SAHs' tests.

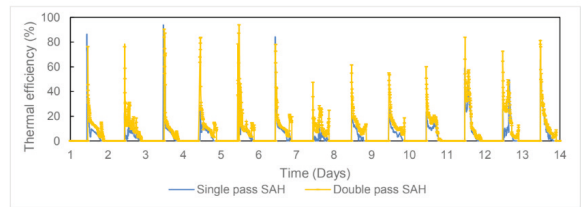


Figure 9. Thermal efficiencies calculated for both SAHs.

## EVALUATION OF THE THERMAL STORAGE MATERIALS

Once the SAH experiments were concluded, the double-pass air heater was connected to the heat storage container. Figure 10 shows the difference in temperature of the air that exits and enters the SAH, using the sand, pebbles and rocks, where it can be observed that the sand in cans gets the higher temperature difference. Using Eq. 9, it was determined that the thermal efficiencies for heat storage were  $0.88$  for sand in aluminium cans,  $0.49$  for pebbles and  $0.48$  for rocks. Considering the results of storage efficiency material and the ease of handling, sand in aluminium cans were selected for sludge drying. These results agree with Subhaschandra Singh et al. (2018), (Subhaschandra Singh et al., 2018) who got a higher thermal storage efficiency using sand in cans than pebbles. Sand used for thermal storage was also observed to increase the operation average temperature at experiments made by (Omara & Kabeel, 2014).

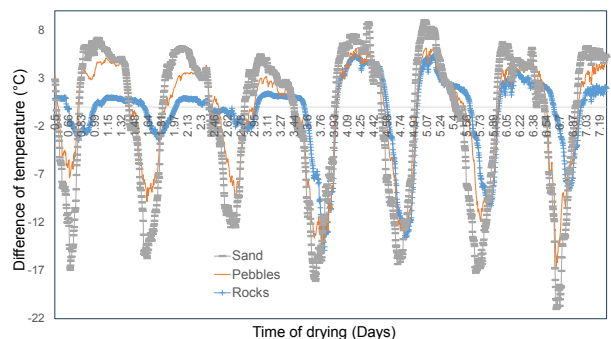


Figure 10. Instant heat flux calculated for each TES material.

Figure 11 shows the results of the change in the moisture of the sludge dried with or without thermal storage. At the beginning of the process, from  $Q_{\text{rad}}$  0 to 16700 kJ/kg, the humidity was reduced faster when thermal storage was not used. Due to the heat, the entrance to the solar dryer was higher, and no part of its heat was stored. However, as can be seen, in the night-time, the trend changed, being faster when it was used thermal storage, showing a remarkable reduction of the moisture ever after before the sunshine, promoting a dried in the non-sunny hours (Andharia et al., 2023), because it was used the stored heat. When the thermal storage device was used, the moisture got a stable value faster than when this device was not used; it was at  $Q_{\text{rad}}$  58384 kJ/kg and 65020 kJ/kg, respectively. These results are in agreement with Bhavsar and Patel (2023) (Bhavsar & Patel, 2023) and Gilago et al., (Gilago et al., 2023) who observed a higher performance of the drying process when was used thermal storage systems due a higher utilisation of the energy (Andharia et al., 2023) and due that the warmer air entering the solar dryer, after the thermal storage system, promotes better dehydration of the material to be dried, as it can remove more moisture from the material (Mathew et al., 2023).

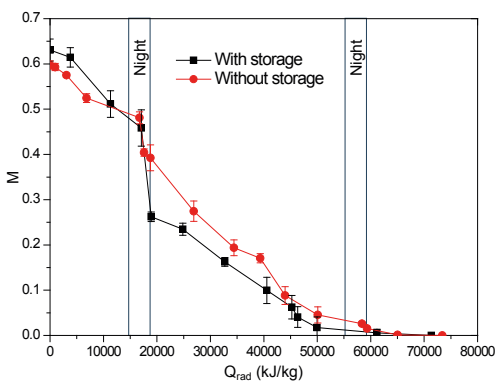


Figure 11. Change in moisture content of samples with and without thermal storage. Error bars symbolise the standard deviation of the results (n=3)

Results show significant differences in the drying process carried out with and without thermal storage, with F values higher than the standardised value ( $10.4 > 1.15 \times 10^{-5}$ ). The Tukey test shows also observed significant differences between the runs.

As observed, the thermal storage system allows the enhanced performance of the solar drying of the aquaculture sludge, even after sunset.

## CONCLUSIONS

In the current research, we evaluated different sizes of fins placed inside a solar air heater, the evaluation of a single-pass and the double-pass of the solar air heater and the evaluation of a thermal storage system to improve the solar drying of a sludge coming from the scallop aquaculture industry. The following are the main conclusions of the outcomes of this study:

Using higher fins in the solar air heater reduces energy consumption. The enhancement is attributed to an increased performance of the solar air heater, which is directly associated with the Nusselt number.

The efficiency of the solar air heater and drying of the sludge depends on the solar radiation and the temperature of the air inside it; also, a high-efficiency dryer allows for removing moisture using lower amounts of energy. When using a solar air heater with fins, it is possible to use a smaller amount of solar energy and a shorter time to get an adequate drying level. The utilisation of the double-pass SAH allows a higher maximum temperature at the exit of the device than when was used the single-pass SAH. Also, the first one got higher thermal efficiency due to the enhancing the heat transfer, allowing a higher utilisation of this heat by the air.

The thermal storage materials evaluation showed that the sand in aluminium cans performs better than pebbles and rocks,

getting a higher difference in the temperature of the air that exits and enters the SAH.

The drying process carried out using thermal storage permits a higher reduction of the moisture of the industrial sludge than when was thermal storage system, promoting a dried process even in non-sunny hours. When thermal storage was used, the humidity got a stable value faster than when this device was not used, observing significant differences

in the drying process carried out with and without thermal storage and significant differences between the runs.

## ACKNOWLEDGEMENTS

The authors thank the Central Laboratory for Marine Aquaculture of the Marine Sciences Department of the Universidad Católica del Norte for providing invaluable equipment support.

## REFERENCES

- Andharia, J. K., Solanki, J. B., & Maiti, S. (2023). Performance evaluation of a mixed-mode solar thermal dryer with black pebble-based sensible heat storage for drying marine products. *Journal of Energy Storage*, *57*, 106186. <https://doi.org/10.1016/J.EST.2022.106186>
- Bannister, J., Sievers, M., Bush, F., & Bloecher, N. (2019). Biofouling in marine aquaculture: a review of recent research and developments. *Biofouling*. <https://doi.org/10.1080/08927014.2019.1640214>
- Bera, A., Trivedi, J. S., Kumar, S. B., Chandel, A. K. S., Haldar, S., & Jewrajka, S. K. (2018). Anti-organic fouling and anti-biofouling poly(piperazineamide) thin film nanocomposite membranes for low pressure removal of heavy metal ions. *Journal of Hazardous Materials*, *343*, 86–97. <https://doi.org/10.1016/J.JHAZMAT.2017.09.016>
- Bhavsar, H., & Patel, C. M. (2023). Performance analysis of cabinet type solar dryer for ginger drying with & without thermal energy storage material. *Materials Today: Proceedings*, *73*, 595–603. <https://doi.org/10.1016/J.MATPR.2022.11.280>
- Comas, J., Parra, D., Balasch, J. C., & Tort, L. (2021). Effects of fouling management and net coating strategies on reared gilthead sea bream juveniles. *Animals*, *11*(3), 1–15. <https://doi.org/10.3390/ani11030734>
- Di Fraia, S., Massarotti, N., Vanoli, L., & Costa, M. (2016). Thermo-economic analysis of a novel cogeneration system for sewage sludge treatment. *Energy*. <https://doi.org/10.1016/j.energy.2016.07.144>
- Gilago, M. C., Mugi, V. R., & V. P., C. (2023). Performance assessment of passive indirect solar dryer comparing without and with heat storage unit by investigating the drying kinetics of carrot. *Energy Nexus*, *9*, 100178. <https://doi.org/10.1016/J.NEXUS.2023.100178>
- Goel, V., Hans, V. S., Singh, S., Kumar, R., Pathak, S. K., Singla, M., Bhattacharyya, S., Almatrafi, E., Gill, R. S., & Saini, R. P. (2021). A comprehensive study on the progressive development and applications of solar air heaters. *Solar Energy*, *229*, 112–147. <https://doi.org/10.1016/J.SOLENER.2021.07.040>
- Jeong, E., Byun, J., Bayarkhuu, B., & Hong, S. W. (2021). Hydrophilic photocatalytic membrane via grafting conjugated polyelectrolyte for visible-light-driven biofouling control. *Applied Catalysis B: Environmental*, *282*, 119587. <https://doi.org/10.1016/J.APCATB.2020.119587>
- Kashyap, T., Thakur, R., Sethi, M., Tripathi, R. K., Thakur, A., Kumar, S., Kumar, P., Goel, B., & Chand, S. (2023). The influence of reflector on the thermal performance of single and double pass solar air heater: A comprehensive review. *Materials Today: Proceedings*, *72*, 1260–1269. <https://doi.org/10.1016/j.matpr.2022.09.297>
- Kluger, L. C., Taylor, M. H., Wolff, M., Stotz, W., & Mendo, J. (2019). From an open-access fishery to a regulated aquaculture business: the case of the most important Latin American bay scallop (*Argopecten purpuratus*). *Reviews in Aquaculture*, *11*(1), 187–203. <https://doi.org/10.1111/raq.12234>
- Kocbek, E., Garcia, H. A., Hooijmans, C. M., Mijatović, I., Lah, B., & Brdjanovic, D. (2020). Microwave treatment of municipal sewage sludge: Evaluation of the drying performance and energy demand of a pilot-scale microwave drying system. *Science of The Total Environment*, *742*, 140541. <https://doi.org/10.1016/J.SCITOTENV.2020.140541>

- Kumar, A., Kumar, R., Maithani, R., Chauhan, R., Kumar, S., & Nadda, R. (2017). An experimental study of heat transfer enhancement in an air channel with broken multi type V-baffles. *Heat and Mass Transfer/Waerme- Und Stoffuebertragung*, 53(12), 3593–3612. <https://doi.org/10.1007/s00231-017-2089-1>
- Kumar, S., Kumar, U., Piyush, Harsh, Chandini, S., Chand, S., Lakshmana Kishore, T., Anandaram, H., Rana, N., & Siddiqui, A. H. (2023). CFD analysis of the influence of distinct thermal enhancement techniques on the efficiency of double pass solar air heater (DP-SAH). *Materials Today: Proceedings*. <https://doi.org/10.1016/J.MATPR.2023.05.454>
- Mathew, A. A., Thangavel, V., Mandhare, N. A., & Nukulwar, M. R. (2023). Latent and sensible heat thermal storage in a heat pipe-based evacuated tube solar dryer: A comparative performance analysis. *Journal of Energy Storage*, 57, 106305. <https://doi.org/10.1016/J.EST.2022.106305>
- Mugi, V. R., Das, P., Balijepalli, R., & VP, C. (2022). A review of natural energy storage materials used in solar dryers for food drying applications. *Journal of Energy Storage*, 49, 104198. <https://doi.org/10.1016/J.EST.2022.104198>
- Nobakht-Kolur, F., Zeinoddini, M., Harandi, M. M. A., Abi, F. A., & Jadidi, P. (2021). Effects of soft marine fouling on wave-induced forces in floating aquaculture cages: Physical model testing under regular waves. *Ocean Engineering*, 238, 109759. <https://doi.org/10.1016/J.OCEANENG.2021.109759>
- Omara, Z. M., & Kabeel, A. E. (2014). The performance of different sand beds solar stills. *International Journal of Green Energy*, 11(3), 240–254. <https://doi.org/10.1080/15435075.2013.769881>
- Pachori, H., Baredar, P., Sheorey, T., Gupta, B., Verma, V., Hanamura, K., & Choudhary, T. (2023). Sustainable approaches for performance enhancement of the double pass solar air heater equipped with energy storage system: A comprehensive review. *Journal of Energy Storage*, 65. <https://doi.org/10.1016/j.est.2023.107358>
- Poblete, R., & Painemal, O. (2018). Solar Drying of Landfill-Leachate Sludge: Differential Results Through the Use of Peripheral Technologies. In *Environmental Progress and Sustainable Energy*. <https://doi.org/10.1002/ep.12951>
- Poblete, R., & Painemal, O. (2020). Improvement of the solar drying process of sludge using thermal storage. *Journal of Environmental Management*, 255(June 2019), 109883. <https://doi.org/10.1016/j.jenvman.2019.109883>
- Poonia, S., Singh, A. K., & Jain, D. (2022). Performance evaluation of phase change material (PCM) based hybrid photovoltaic/thermal solar dryer for drying arid fruits. *Materials Today: Proceedings*, 52, 1302–1308. <https://doi.org/10.1016/J.MATPR.2021.11.058>
- Prachayawarakorn, S., Tia, W., Plyto, N., & Soponronnarit, S. (2008). Drying kinetics and quality attributes of low-fat banana slices dried at high temperature. *Journal of Food Engineering*. <https://doi.org/10.1016/j.jfoodeng.2007.08.011>
- Prakash, O., Kumar, A., Samsher, Dey, K., & Aman, A. (2022). Exergy and energy analysis of sensible heat storage based double pass hybrid solar air heater. *Sustainable Energy Technologies and Assessments*, 49, 101714. <https://doi.org/10.1016/J.SETA.2021.101714>
- Ramajo, L., Valladares, M., Astudillo, O., Fernández, C., Rodríguez-Navarro, A. B., Watt-Arévalo, P., Núñez, M., Grenier, C., Román, R., Aguayo, P., Lardies, M. A., Broitman, B. R., Tapia, P., & Tapia, C. (2020). Upwelling intensity modulates the fitness and physiological performance of coastal species: Implications for the aquaculture of the scallop *Argopecten purpuratus* in the Humboldt Current System. *Science of The Total Environment*, 745, 140949. <https://doi.org/10.1016/J.SCITOTENV.2020.140949>
- Rezaei, M., Sefid, M., Almutairi, K., Mostafaeipour, A., Ao, H. X., Hosseini Dehshiri, S. J., Hosseini Dehshiri, S. S., Chowdhury, S., & Techato, K. (2022). Investigating performance of a new design of forced convection solar dryer. *Sustainable Energy Technologies and Assessments*, 50, 101863. <https://doi.org/10.1016/J.SETA.2021.101863>
- Saravanakumar, P. T., Somasundaram, D., & Matheswaran, M. M. (2019). Thermal and thermo-hydraulic analysis of arc shaped rib roughened solar air heater integrated with fins and baffles. *Solar Energy*, 180, 360–371. <https://doi.org/10.1016/J.SOLENER.2019.01.036>
- Saravanakumar, P. T., Somasundaram, D., & Matheswaran, M. M. (2020a). Exergetic investigation and optimization of arc shaped rib roughened solar air heater integrated with fins and baffles. *Applied Thermal Engineering*, 175, 115316. <https://doi.org/10.1016/J.APPLTHERMALENG.2020.115316>

- Saravanakumar, P. T., Somasundaram, D., & Matheswaran, M. M. (2020b). Exergetic investigation and optimization of arc shaped rib roughened solar air heater integrated with fins and baffles. *Applied Thermal Engineering*, 175, 115316. <https://doi.org/10.1016/J.APPLTHERMALENG.2020.115316>
- Singh, P. P., Singh, S., & Dhaliwal, S. S. (2006). Multi-shelf domestic solar dryer. *Energy Conversion and Management*. <https://doi.org/10.1016/j.enconman.2005.10.002>
- Singh, S., & Negi, B. S. (2020). Numerical thermal performance investigation of phase change material integrated wavy finned single pass solar air heater. *Journal of Energy Storage*, 32, 102002. <https://doi.org/10.1016/J.EST.2020.102002>
- Straume, H. M., Anderson, J. L., Asche, F., & Gaasland, I. (2020). Delivering the goods: The determinants of Norwegian seafood exports. *Marine Resource Economics*, 35(1), 83–96. <https://doi.org/10.1086/707067>
- Subhaschandra Singh, T., Nath Verma, T., Jahiya, M., Keny Singh, P., Kheiruddin, M., Ajitkumar, K., Wilson Singh, N., & Dhanadash Singh, H. (2018). Forced Convective Solar Air Heater: Effect of Thermal Storage Materials. In *International Journal of Applied Engineering Research* (Vol. 13, Issue 8). <http://www.ripublication.com>
- Surendhar, G., Srinivasan, G., Muthukumar, P., & Senthilmurugan, S. (2021). Performance analysis of arc rib fin embedded in a solar air heater. *Thermal Science and Engineering Progress*, 23, 100891. <https://doi.org/10.1016/J.TSEP.2021.100891>
- Surendhar, G., Srinivasan, G., Muthukumar, P., & Senthilmurugan, S. (2022). Investigation of thermal performance in a solar air heater having variable arc ribbed fin configuration. *Sustainable Energy Technologies and Assessments*, 52, 102069. <https://doi.org/10.1016/J.SETA.2022.102069>
- Wang, P., Mohammed, D., Zhou, P., Lou, Z., Qian, P., & Zhou, Q. (2019). Roof solar drying processes for sewage sludge within sandwich-like chamber bed. *Renewable Energy*. <https://doi.org/10.1016/j.renene.2018.09.081>
- Yadav, A. S., Gupta, S., Agrawal, A., Saxena, R., Agrawal, N., & Nashine, S. (2022). Performance enhancement of solar air heater by attaching artificial rib roughness on the absorber Plate. *Materials Today: Proceedings*, 63, 706–717. <https://doi.org/10.1016/J.MATPR.2022.05.064>